Cryogen Spray Cooling Efficiency: Improvement of Port Wine Stain Laser Therapy Through Multiple-Intermittent Cryogen Spurts and Laser Pulses

Guillermo Aguilar, PhD,[1,2]* Sergio H. Díaz, PhD,[2] Enrique J. Lavernia, PhD,[1,3] and J. Stuart Nelson, MD, PhD[1,2]
[1]*Center for Biomedical Engineering, University of California, Irvine, California 92697*
[2]*Beckman Laser Institute, University of California, Irvine, California 92612*
[3]*Department of Chemical Engineering and Materials Science, University of California, Irvine, California 92697*

Background and Objectives: Cryogen spray cooling (CSC) is used to minimize the risk of epidermal damage during laser treatment of port wine stain (PWS) birthmarks. Unfortunately, CSC may not provide the necessary protection for patients with high concentrations of epidermal melanin. The objectives of this study are to: (1) provide a definition of cooling efficiency (η) based on the amount of heat removed per unit area of skin for a given cooling time; (2) using this definition, establish the η of previously reported spray nozzles; (3) identify the maximum benefit expected in PWS laser therapy based solely on improvement of η; and (4) study the feasibility of using multiple-intermittent cryogen spurts and laser pulses to improve PWS laser therapy.

Study Design/Materials and Methods: A theoretical definition to quantify η is introduced. Subsequently, finite difference heat diffusion and Monte Carlo light distribution models are used to study the spatial and temporal temperature distributions in PWS skin considering: (1) the current approach to PWS laser therapy consisting of a single cryogen spurt followed by a single pulsed dye laser exposure (SCS-SLP approach); and (2) multiple cryogen spurts and laser pulses (MCS-MLP approach). At the same time, an Arrhenius-type kinetic model is used to compute the epidermal and PWS thermal damages (Ω_E and Ω_{PWS}, respectively) for a high epidermal melanin concentration (20%), corresponding to skin types V–VI.

Results: The η corresponding to a wide range of heat transfer coefficients (h) is quantified. For reported CSC nozzle devices η varies from 40 to 98%. Using the SCS-SLP approach, it is shown that even $\eta = 100\%$ cannot prevent excessive Ω_E for a skin types V–VI. In contrast, the MCS-MLP approach provides adequate epidermal protection while permitting PWS photocoagulation for the same skin types.

Conclusions: The new proposed definition allows to compute the cooling efficiency of CSC nozzle devices. Computer models have been developed and used to show that the SCS-SLP approach will not provide adequate epidermal protection for darker skin patients (skin types V–VI), even for $\eta = 100\%$. In contrast, the MCS-MLP approach may be a viable solution to improve PWS laser therapy for darker skin patients. Lasers Surg. Med. 31:27–35, 2002.

Key words: Arrhenius kinetic model; cooling selectivity; heat diffusion model; sequential cryogen pulses; Monte Carlo; thermal confinement; thermal tissue damage

INTRODUCTION

Cryogen spray cooling (CSC) has been used effectively during laser therapy to cool selectively the most superficial layers of skin (tens of micrometers deep), while minimally affecting deeper targets such as port wine stain (PWS) birthmarks (150–500 μm deep) [1,2]. Clinical studies [2–4] have demonstrated that radiant exposures of 8–9 J/cm^2 are required to cause irreversible photocoagulation of PWS vessels in patients with higher epidermal melanin concentration (i.e., skin types V–VI, according to Fitzpatrick classification [5]). Unfortunately, the current approach to PWS laser therapy—consisting of a single cryogen spurt and a single laser pulse (SCS-SLP approach)—does not provide sufficient epidermal protection for patients with darker skin types. Consequently, radiant exposures are still limited to avoid non-specific thermal injury. To solve this problem, recent studies have sought to optimize cryogen spurt durations to maximize the temperature difference between the epidermis and PWS vessels [6,7]. Other studies have focused on increasing the rate of the heat extraction through the skin surface (q) by different means, such as variation of nozzle diameter [8,9], nozzle-to-skin distance [10,11], control of cryogen deposition [12], and enhancement of cryogen film evaporation [13]. In general, it has been concluded that cryogen spurts of 100–250 milliseconds result in better epidermal protection than that provided by 30–50 milliseconds spurts—which most physicians still use, while the increase in q by all these means appears to be moderate. Despite all these efforts, CSC efficiency (η) has not yet been defined. Therefore, it

Grant sponsor: Institute of Arthritis and Musculoskeletal and Skin Diseases at the National Institutes of Health; Grant number: AR43419.
*Correspondence to: Guillermo Aguilar, PhD, Beckman Laser Institute and Medical Clinic, 1002 Health Sciences Road East, Irvine, CA 92612-1475. E-mail: gaguilar@bli.uci.edu
Accepted 4 April 2002
Published online in Wiley InterScience (www.interscience.wiley.com).
DOI 10.1002/lsm.10076

remains unclear how efficient current CSC devices are and, also, what improvement in PWS therapy can be expected based solely on CSC maximization.

Besides these studies on CSC, other alternatives for improving PWS laser therapy have been investigated. For instance, Tan et al. [14] studied the effect of 450 microseconds multiple pulses using a 577 nm dye laser and they concluded that multiple pulses did not increase the depth of vascular injury. However, each pulse was delivered sequentially to the same site at intervals of 3 seconds, which was far too long to preserve thermal confinement. Anvari et al. [15,16] proved the utility of applying intermittent cryogen spurts along with continuous laser irradiation to cause deeper tissue photocoagulation using a Nd:YAG laser. However, the absorption coefficients of melanin and hemoglobin are very small at 1064 nm compared to those corresponding to laser wavelengths used for the treatment of PWS (e.g., $\lambda = 585–595$ μm).

In the present study, we introduce the concept of cooling efficiency (η) applicable to CSC procedures of duration τ_c, and calculate η for a wide range of heat transfer coefficient (h) values, including those reported for various CSC devices. We then simulate a single cryogen spurt followed by a single laser pulse (SCS-SLP approach) using computer models of heat diffusion, light distribution, and tissue damage and investigate what is the necessary η required to obtain a safe and effective treatment for PWS patients with darker skin types. Finally, using these computer models we study the use of multiple cryogen spurts applied intermittently with multiple laser pulses (MCS-MLP approach) to improve PWS laser therapy. The rationale behind the latter study is that: (1) the energy deposited in PWS vessels by each laser pulse is greater than that lost by diffusion between two consecutive pulses; and (2) cryogen spurts applied intermittently with laser pulses maintain the epidermal temperature below the threshold for thermal damage.

METHODS AND PROCEDURES

Definition of Cooling Efficiency

The following definition is proposed to quantify skin cooling efficiency (η):

$$\eta = \frac{Q(\tau_c)}{Q_{\max}(\tau_c)} \times 100, \tag{1}$$

where $Q(\tau_c)$ represents the amount of heat removed per unit area of skin in a given cooling time τ_c, and $Q_{\max}(\tau_c)$ is the theoretical maximum amount of heat that can be removed in the same time.

At the skin surface, a Robin boundary condition is used, which is reasonable considering the convective and evaporative effects of CSC. Under these circumstances, $Q(\tau_c)$ may be computed as:

$$Q(\tau_c) = \int_0^{\tau_c} h(t)[T_s(t) - T_c(t)]dt, \tag{2}$$

where $h(t)$ represents the heat transfer coefficient at the sprayed surface; $T_s(t)$, the skin surface temperature; and $T_c(t)$, the temperature of the cryogen layer on the surface. $Q_{\max}$ results when $h \to \infty$ and, therefore, is given by:

$$Q_{\max}(\tau_c) = \lim_{h\to\infty} \int_0^{\tau_c} h(t)[T_s(t) - T_c(t)]dt. \tag{3}$$

Inspection of Equations 2 and 3 indicates that in order to compute Q and $Q_{\max}$, we must select a value of τ_c in addition to three other parameters, namely, $T_c(t)$, $h(t)$, and $T_s(t)$, which may be determined either experimentally or by reasonable theoretical assumptions. In the section that follows, the rationale for selecting these parameters is justified.

Selection of Parameters [τ_c, $T_c(t)$, $h(t)$, and $T_s(t)$]

Based on the work of Verkruysse et al. [6] and Tunnell et al. [7], which indicates that cryogen spurts of at least 100 milliseconds provide better cooling selectivity, we select three cooling times, τ_c, for the present study: 100, 200, and 300 milliseconds.

To provide an estimate of T_c, we use the average steady-state spray temperature as measured by inserting bare miniature thermocouples (300 μm bead diameter) into the center of tetrafluoroethane (refrigerant R-134a) sprays. These sprays are produced by atomizing nozzles as cryogen is released from a pressurized container at 6.7 bar (its saturation pressure at room temperature) to the atmosphere. Based on systematic experiments, we have determined that the average spray temperature reaches a minimum between −55 and −62°C, regardless of nozzle position [11], geometry [10,17], and relative humidity [10,18] and, therefore, we choose a value −60°C to represent a constant T_c for this study.

As with T_c, we choose a constant h value to represent the boundary condition at the sprayed surface during a given simulation. Nine different values of h, ranging from 1,000 to 100,000 W/m^{2}K are used, namely: 1,000–5,000 in increments of 1,000, plus 10,000, 30,000, 60,000, and 100,000 W/m^{2}K (Table 1). This broad range includes experimentally measured values reported in the literature [8,9,11,19–21], and the upper limit represents the case for $h \to \infty$, which is needed to compute η by Equation 1. The wide range in the h values reported by different investigators is mainly attributed to differences in experimental conditions such as nozzle geometry, spraying distance, and ambient humidity, but also, measurement technique.

TABLE 1. Heat Transfer Coefficients (h) Used in This Study

h [W/(m^2 K)]	Similar values reported in	Substrate
1,000	Arbitrary minimum value	
2,000–3,000	Torres et al. [20]	Epoxy block
4,000–8,500	Aguilar et al. [11,21]	Copper disc
10,000–60,000	Verkruysse et al. [8]	Epoxy block, Copper rod
	Aguilar et al. [9]	Copper rod
	Anvari et al. [19]	Human skin
100,000	Arbitrary maximum value	

Under the assumptions mentioned above, i.e., fixed τ_c, and constant T_c and h, it is possible to determine $T_s(t)$ from the exact solution to the heat conduction equation for a semi-infinite medium, subject to a Robin boundary condition [22] or, alternatively, from a finite-difference (FD) approximation to this equation. In the section that follows, we describe the details of computer models for heat diffusion, light distribution, and tissue damage evaluation developed for this study.

Finite Difference Model

To study the combined effect of CSC and laser irradiation, we model human skin as an axi-symmetric, semi-infinite cylinder composed of four layers (Fig. 1): an epidermal melanin layer, a dermis layer, a PWS layer, and a deeper dermis layer below the PWS. Using a 2D forward-time central space FD approximation to the heat diffusion equation, we compute the spatial and temporal distribution of skin temperature during CSC and after laser exposure. Because of the axi-symmetric geometry, only half of the skin cross-section below the sprayed and irradiated area is discretized and used for the computations (shaded areas of Fig. 1). This skin cross section is 15 mm wide by 1 mm thick and is discretized into 60 and 100 nodes, respectively. Considering the tissue thermal properties and the range of values of the boundary condition to be studied, time steps of 100 microseconds ensure stability and convergence criteria.

The skin layers' thickness, and thermal and optical properties used in this study are listed in Table 2. The optical properties correspond to a 585 nm wavelength, and they are the same reported and used in previous studies [21, 23–25]. For simplicity, it is further assumed that both chromophores of interest, melanin and hemoglobin, have a homogeneously spatial distribution within the epidermis and PWS, respectively. For all simulations, we use a single epidermal absorption coefficient of 80 cm^{-1}, corresponding to melanin volume fraction, v_{fm}, of 20% (skin types V–VI) assuming a melanosome absorption coefficient of 400 cm^{-1} at 585 nm [26]. We also use an effective PWS layer absorption coefficient of 19.1 cm^{-1}, corresponding to a vasculature volume fraction, v_{fb}, of 10% [27]. It is worthy of mention that the relationship between v_{fm} and the Fitzpatrick skin type classification mentioned above is only a rough approximation intended to give clinicians a better insight for the skin type selected for this study, and is based on reported values of melanosomes distribution within the epidermis [28] and experience [29].

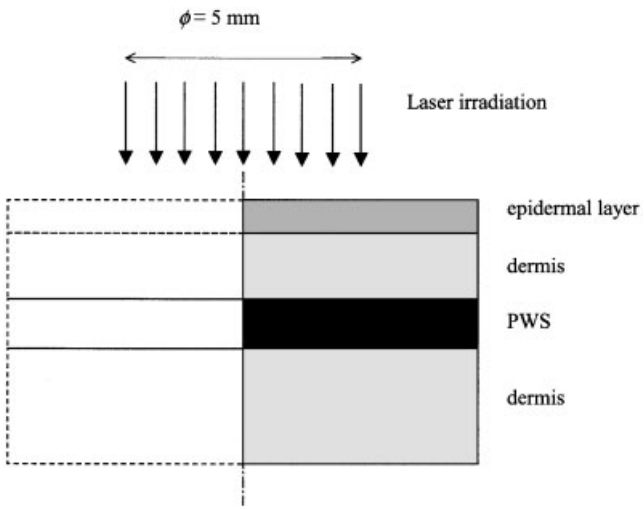

Fig. 1. Four-layer model used in the numerical simulation. The shaded areas represent the discretized cross section, which consists of 15 mm in the radial direction and 1 mm in the axial direction discretized into 60 and 100 nodes, respectively.

A 2D model is selected for this study for two main reasons. The first is that MCML/CONV uses the shape and diameter of the laser beam to compute a 2D light distribution and, thus, introduces lateral variations of the light distribution and, the second and most important, is that this model was developed with the idea to study other aspects of PWS laser therapy, such as the influence of lateral variations of the heat flux at the boundary on the epidermal thermal damage (Ω_E), which will require the use of a second dimension.

CSC, Laser Irradiation, and Tissue Thermal Damage

Single cryogen spurt and single laser pulse (SCS-SLP). Starting with a constant skin temperature $T_0 = 30°C$, the temperature distribution resulting after a SCS-SLP approach is computed by imposing a Robin boundary condition at the skin surface with constant T_c and h values. No delay is allowed between the end of the spurt and the beginning of laser exposure. To simulate the effect of laser-induced heating within tissue, we use the 2D Monte Carlo Multi Layer (MCML) code developed by Wang et al. [30]. The adjunct program to MCML, CONV [31], is used to take the infinitesimally narrow photon beam from the MCML simulations and create a flat top, circular beam with 5-mm diameter. All MCML/CONV simulations use 100,000 photons. Then, the heat source term generated using MCML/CONV is incorporated into the FD heat diffusivity equation to simulate absorption of laser energy by the tissue. The pulse duration (τ_l) is fixed at 1.5 microsecond for all simulations.

To compute epidermal and PWS thermal damages, Ω_E and Ω_{PWS}, respectively, we use an Arrhenius-type kinetic model given by Equation 4:

$$\Omega(t) = \int_0^t A \exp(-E_a/RT)dt \tag{4}$$

where A is a frequency factor [1/s], E_a an activation energy barrier [J/mole], R the universal gas constant (8.32 J/mole K), and T the absolute temperature [K]. The empirical values for A and E_a are the same as those used in previous studies [21,25], listed in Table 3. The computations of Ω_E and Ω_{PWS} are incorporated into the FD heat diffusivity model and calculated for each time step and for

TABLE 2. Thickness, Thermal, and Optical Properties of Layers Used With the FD Heat Diffusion and MCML/CONV Models

	Layer			
Properties	Epidermis	Dermis	Blood	Dermis below PWS
Thickness [μm]	50	150,250	20,050	$\gg$ 1,000
k [W/(m K)]	0.21	0.53	0.55	0.53
ρ [kg/m^3]	1,200	1,200	1,100	1,200
c [J/(kg K)]	3,600	3,800	3,600	3,800
α [m^2/sec]	4.86×10^{-8}	1.16×10^{-7}	1.39×10^{-7}	1.16×10^{-7}
μ_a [cm^{-1}]	80	2.4	19.1	2.4
μ_s [cm^{-1}]	470	129	467	129
g	0.79	0.79	0.99	0.79
n	1.37	1.37	1.33	1.37

all grid points of the left boundary, i.e., along the symmetry axis of the sprayed/irradiated area. Values of Ω_E and Ω_{PWS} reported in this study correspond to the depths where maximal thermal damage occurred. Excessive damage is considered to occur when a value for Ω_E is higher than 1, which corresponds to a 63% decrease from the original total of undamaged tissue constituents. If this critical value is reached, the program warns about excessive tissue damage and stops. Otherwise, computations are carried out for one more second after laser exposure. Beyond that time, it is verified that both Ω_E and Ω_{PWS} do not change significantly.

At the end of laser exposure, the boundary condition used during CSC is modified by imposing an $h = 100$ W/m^{2}K and $T_c = 0^\circ$C, which presumably simulates the presence of a thin layer of water and ice that slowly evaporates [18].

Multiple Cryogen Spurts and Laser Pulses (MCS-MLP)

Bearing in mind the limitations of the SCS-SLP approach, we decided to study the possibility of inducing higher temperatures within the PWS while preserving the epidermis. We achieve this through an appropriate combination of multiple cryogen spurts applied intermittently with multiple laser pulses (MCS-MLP approach). The rationale behind this approach is that the temperature of PWS vessels can be gradually increased if the energy deposited within them by each pulse is larger than that lost by heat diffusion between two consecutive pulses, i.e., if thermal confinement is preserved. To achieve this requirement, MCS-MLP should be applied intermittently so that the epidermal temperature does not exceed the threshold for thermal damage. Figure 2 shows a schematic of a sequence of cryogen spurts and laser pulses used in this study.

TABLE 3. Arrhenius Damage Process Coefficients

	A [1/sec]	E_a [J/mole]
Bulk skin	7.6×10^{76}	550,000
Hemoglobin	7.6×10^{66}	455,000

The appropriate repetition rate can be roughly approximated based on the thermal time constant of each absorbing layer (t_E and t_{PWS}), which may be approximated by $t_E = (\rho c L)/h$ and $t_{PWS} = L^2/\alpha$ for the epidermis and PWS, respectively. Here ρ, c, h, L, and α represent epidermal density, epidermal specific heat, skin surface heat transfer coefficient, layer thickness, and PWS thermal diffusivity, respectively (see Tables 1 and 2 for values). The average epidermal layer is about 50 μm thick (as used for this study) and assuming $h = 10{,}000$ W/m^{2}K, $t_E \cong 22$ milliseconds. A 3D reconstruction of PWS published by Smithies et al. [32] shows multiple clusters of blood vessels that span down to 1.3 mm below the epidermal-dermal junction. Most importantly, almost all the blood volume fraction is contained within this junction and 500 μm below. Therefore, to represent this vasculature by a single layer, we have used a PWS vessel cluster 200 μm thick and 200 μm deep, for which $t_{PWS} \cong 284$ milliseconds. If a series of cryogen spurts are applied onto the skin surface with a frequency of $\sim 1/t_E$, most of the heat generated within the epidermis by each laser pulse can be removed during the subsequent cryogen spurt, while only $\sim 16\%$ of the heat generated within the PWS would be conducted out in the same time. Therefore, multiple laser pulses gradually increase PWS temperature, while the multiple-intermittent cryogen spurts cool and protect the epidermis.

Using the numerical models described above, we simulate a MCS-MLP approach and compute the skin temperature profiles and Ω_E and Ω_{PWS} for the skin types selected for this study (V–VI). We consider two configurations: (1) PWS vessel cluster 200 μm deep and 200 μm thick (as for the SCS-SLP case described above); and (2) PWS vessel 300 μm deep and 50 μm thick. In this case, $t_{PWS} \sim 18$ milliseconds is of the same order of magnitude as t_E (~22 milliseconds) and, therefore, this scenario represents a limiting condition for the minimum vessel size that may be effectively coagulated using this procedure. In both configurations, the initial cryogen spurt is fixed at 100 milliseconds, immediately followed by a 1.5 milliseconds laser pulse.

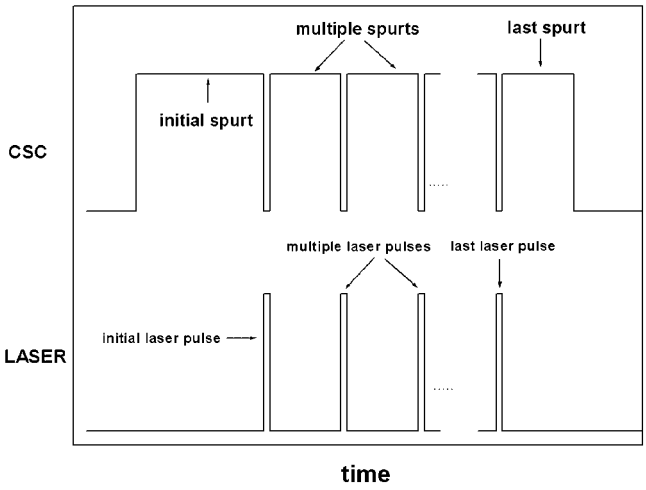

Fig. 2. Schematic of multiple cryogen spurts and laser pulses (MCS-MLP).

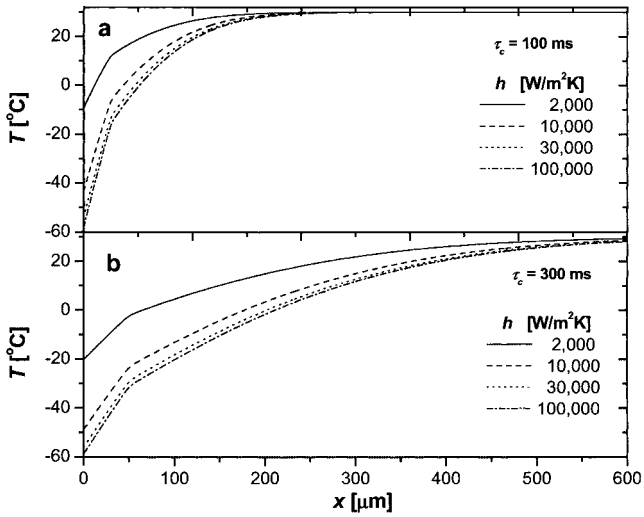

Fig. 3. Temperature profiles as a function of depth computed by the heat diffusivity model using $T_c = -60^\circ$C and h values of: 2,000, 10,000, 30,000, and 100,000 W/m^{2}K. **a**: Profiles for $\tau_c = 100$ milliseconds, and (**b**) $\tau_c = 300$ milliseconds.

Then, multiple cryogen spurts with the same boundary condition values as the initial spurt are alternately applied with laser pulses. Since the 1.5 milliseconds laser pulses are too short compared to the spurt duration, the boundary conditions during the laser pulses remain unchanged. After the last cryogen spurt, the values of T_c and h are fixed at 0°C and 100 W/m^{2}K, respectively. Similarly, Ω_E and Ω_{PWS} are computed simultaneously for each time step and, if the maximum permissible epidermal damage ($\Omega_E = 1$) is not reached, the computations are carried out until 1 second after the end of the last cryogen spurt.

RESULTS

Temperature Profiles, Heat Removed, and CSC Efficiencies

Figure 3a,b show the computed temperature profiles along the axis of symmetry of the sprayed area (left boundary of the discretized human skin model) at the end of 100 and 300 milliseconds cryogen spurts, respectively. Each of the four profiles shown in each figure is computed using the same value for $T_c = -60^\circ$C, and different values of h: 2,000, 10,000, 30,000, and 100,000 W/m^{2}K, respectively. For both values of τ_c computed, $h \geq 30{,}000$ W/m^{2}K is a sufficiently large heat transfer coefficient, beyond which it is almost impossible to induce any further reduction in skin temperature, as suggested by the temperature profiles for $h = 30{,}000$ and 100,000 W/m^{2}K, which are almost identical. Also note the changes in slope at $x = 50$ μm for all profiles. This is due to the difference in the thermal properties between the epidermis and dermis. In fact, these temperature profiles vary significantly from those that assume homogeneous skin thermal properties, as described by Pfefer et al. [25].

Figure 4a shows $Q(\tau)$ computed from Equation 2 for all values of h listed in Table 1 for each value of τ_c used in the present study (100, 200, and 300 microseconds). As expected from Equation 2, $Q(\tau)$ increases with increasing h and τ_c, and it reaches an asymptotic value, which we use to compute $Q_{max}(\tau)$, according to Equation 3. Figure 4b shows η computed using Equation 1. With this definition it is now possible to establish that the η corresponding to reported h values of various CSC nozzle devices varies from 40 [20] to 98% [8].

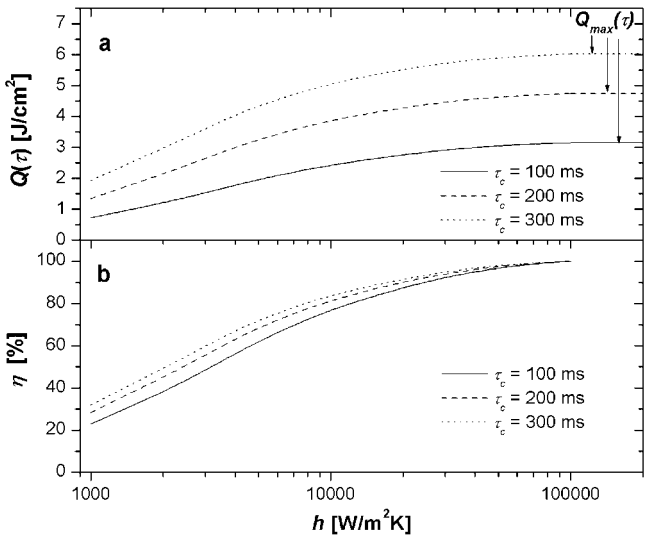

Fig. 4. **a**: Amount of heat removed (Q) by a single cryogen spurt for all values of h listed in Table 1. **b**: Cryogen spray cooling (CSC) efficiencies (η) computed using Equation 1 for all values of h listed in Table 1. The solid curves correspond to cooling time, τ_c, of 100 milliseconds; the dashed curves to $\tau_c = 200$ milliseconds; and the dotted curves to $\tau_c = 300$ milliseconds.

SCS-SLP Approach

Figure 5 shows examples where the SCS-SLP approach would provide inadequate epidermal protection for a patient with skin types V–VI ($v_{fm} = 20\%$, $\mu_a = 80$ cm^{-1}), regardless of η and τ_c. Solid curves represent computed temperature profiles after a 100 milliseconds cryogen spurt and at the end of a 1.5 milliseconds laser pulse ($t = 101.5$ milliseconds) of 6 J/cm^2. Dashed curves represent the computed temperature profiles after a 300 milliseconds cryogen spurt and at the end of a 1.5 milliseconds laser pulse ($t = 301.5$ milliseconds) using the same fluence. The same values of $T_c = (60^\circ$C and $h = 100{,}000$ W/m^{2}K are used in both examples ($\eta = 100\%$). Values for Ω_E and Ω_{PWS} are also shown in Figure 5. Note that even for an ideal situation where $\eta = 100\%$, severe epidermal damage would occur for these skin types, while Ω_{PWS} would be negligible. This example suggests that even though enhancement in η may help to improve the outcome for patients with skin types I–IV, skin thermal resistance may prevent the successful implementation of the SCS-SLP approach for patients with darker skin types V–VI, even if it was possible to attain $\eta = 100\%$.

MCS-MLP Approach

Figure 6a shows computed temperature profiles as a function of depth at the end of the initial cryogen spurt ($t = 100$ milliseconds) and at the end of multiple 60 milliseconds cryogen spurts numbers 1, 4, 8, and 12. Note that except for the profile corresponding to the initial 100 milliseconds spurt, all others follow the corresponding laser pulse shown in Figure 6b and, therefore, the skin temperature is gradually increased. Values of $T_c = -60^\circ$C and $h = 10{,}000$ W/m^{2}K are used for the boundary condition. Figure 6b shows computed temperature profiles as a function of depth at the end of the initial 1.5 milliseconds laser pulse and the end of multiple pulses numbers 1, 4, 8, and 12. A fluence of 4 J/cm^2 is used for all laser pulses. The final values for Ω_E and Ω_{PWS} computed until 1 second after the end of the last cryogen spurt are also shown in Figure 6b.

Finally, we present in Figure 7a,b a similar example for skin types V–VI, with a PWS vessel 50 μm thick and

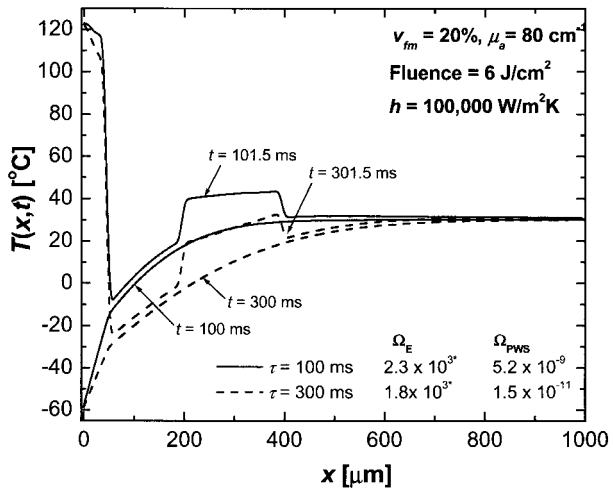

Fig. 5. Temperature profile simulations as a function of depth for skin types V–VI ($v_{fm} = 20\%$, $\mu_a = 80$ cm^{-1}). Solid curves represent temperature profiles after a 100 milliseconds spurt and at the end of a laser pulse (101.5 milliseconds) for $T_c = -60^\circ$C and $h = 100{,}000$ W/m^{2}K. Dashed curves represent temperature profiles after a 300 milliseconds spurt and at the end of a laser pulse (301.5 milliseconds) for the same values of T_c and h. Fluence = 6 J/cm^2. * Denotes maximal Ω_E was reached.

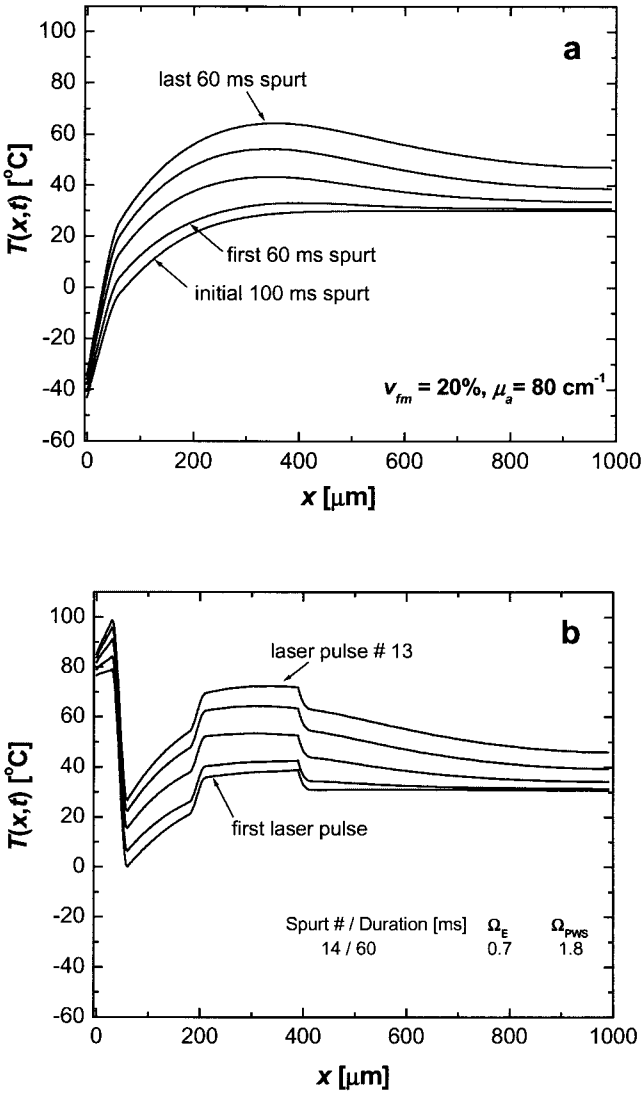

Fig. 6. **a**: Temperature profiles as a function of depth after the initial 100 milliseconds spurt and after the 1st, 4th, 8th, and 12th multiple 60 milliseconds spurts are applied to skin types V–VI ($v_{fm} = 20\%$, $\mu_a = 80$ cm^{-1}) with port wine stain (PWS) vessel cluster 200 μm thick and 200 μm deep. $T_c = -60^\circ$C and $h = 10{,}000$ W/m^{2}K. **b**: Temperature profiles at the end of the first 1.5 milliseconds laser pulse and the end of 1st, 4th, 8th, and 12th multiple laser exposures. Fluence = 4 J/cm^2.

300 μm deep. For this example, a total of 23 additional cryogen spurts/laser pulses were needed to induce a significant Ω_{PWS} while keeping Ω_E below the specified threshold. Figure 7a shows computed temperature profiles as a function of depth at the end of the initial cryogen spurt ($t = 100$ milliseconds) and multiple 50 milliseconds cryogen spurts numbers 1, 10, 20, and 23. Values of $T_c = (60°C$ and $h = 30{,}000$ W/m^{2}K are used for the boundary condition. Figure 7b shows computed temperature profiles as a function of depth at the end of the initial 1.5 milliseconds laser pulse and the end of multiple pulses numbers 1, 10, 20, and 23. A fluence of 4 J/cm^2 is used for all laser pulses.

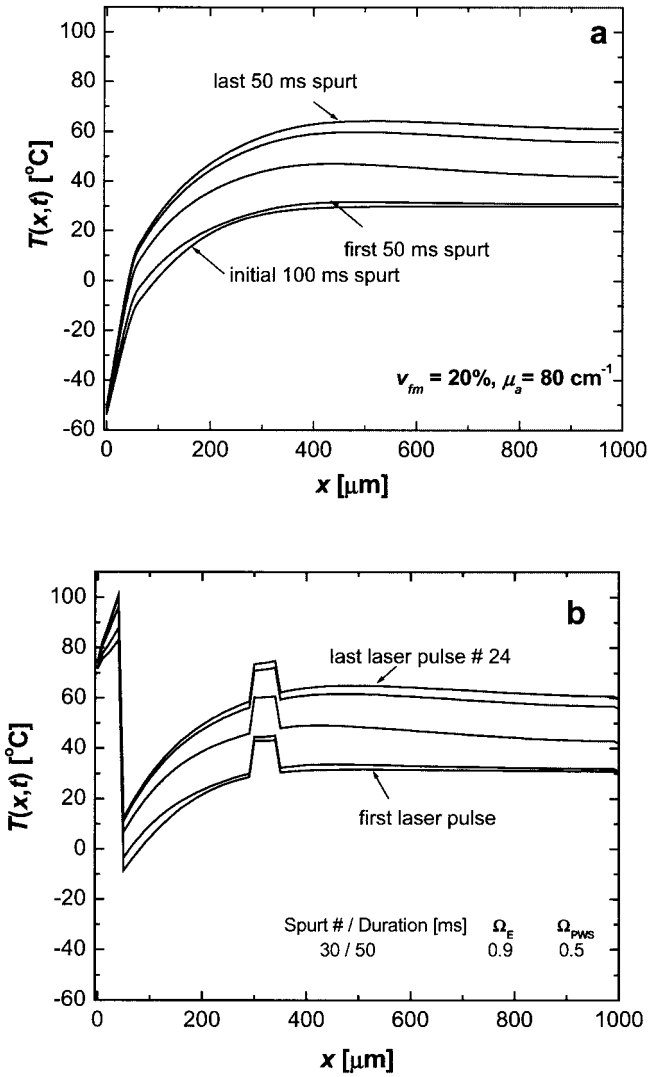

Fig. 7. **a**: Temperature profiles as a function of depth after the initial 100 milliseconds spurt and after the 1st, 10th, 20th, and 23rd multiple 50 milliseconds spurts are applied to skin types V–VI ($v_{fm} = 20\%$, $\mu_a = 80$ cm^{-1}) with PWS vessel 50 μm thick and 300 μm deep. $T_c = (-60°C$ and $h = 30{,}000$ W/m^{2}K. **b**: Temperature profiles at the end of the first 1.5 milliseconds laser pulse and the end of 1st, 10th, 20th, and 23rd multiple laser exposures. Fluence = 4 J/cm^2.

Note that for both examples, additional cryogen spurts intermittently applied with sub therapeutic laser pulses are adequate to induce a significant Ω_{PWS}, while keeping Ω_E below the specified threshold. Also note that these are the same skin types which could not be sufficiently protected with a single cryogen spurt of $\tau_c = 100$ and 300 milliseconds, even with $\eta = 100\%$.

DISCUSSION

Several assumptions had to be made when selecting the CSC parameters for this study. The first assumption was that most of the heat extracted from skin is removed during spray deposition, so that the cooling time, τ_c, is equal to the spurt duration. This simplification is especially true when the laser pulse follows immediately at the end of the cryogen spurt (as in the present study), i.e., no delay is allowed between the cryogen spurt and laser pulse and, therefore, the heat absorbed by the epidermis enhances the evaporation of the remaining pool of liquid cryogen [18]. We also assumed a constant value of T_c, which may not necessarily represent the real cryogen layer temperature because of the enhanced convection and evaporation of the liquid cryogen in contact with the thermocouple bead. Most importantly, our recent studies suggest that T_c and h may vary significantly over time and across the sprayed area [8,9,12] and, therefore, lead to instantaneous and lateral variations in heat flux during cryogen spurts. By using two miniature thermocouples embedded 90 μm below the surface of an epoxy block, and positioned at the center and 3 mm away of the sprayed area, respectively, we have measured temperature differences as large as 12°C [8] during 100 milliseconds spurts. This suggests that heat flux variations may occur across the sprayed area during CSC and, if these variations are large, they could lead to inadequate epidermal protection at certain locations across the irradiated area. We are presently conducting systematic experiments to measure instantaneous and local values of h and T_c produced by nozzles with different geometries.

Figure 3a,b illustrate the effects of h and τ_c on the temperature distributions within the human skin model. For high values of h, for example, $h \geq 30{,}000$ W/m^{2}K, the effect of τ_c on the epidermal temperature is minimal. The reason for this is that once the thermal resistance at the boundary becomes too low relative to the skin thermal resistance, i.e., h becomes too high, the skin thermal resistance physically limits the amount of heat extracted per unit time. This suggests that even if it were possible to reach $\eta = 100\%$, the SCS-SLP approach to PWS laser therapy may not provide sufficient epidermal protection for patients with darker skin types.

A Robin boundary condition with $h \to \infty$ is equivalent to the use of a boundary condition of the first kind (i.e., constant temperature), which is applicable to the case of skin contact cooling (SCC) with a sapphire plate. Based on the definition of η given by Equation 1, it may appear at first inspection that the SCC procedure has $\eta = 100\%$. However, the definition of η requires specification and/or

computation of τ_c and T_s, which are different for SCC and CSC. Typically, SCC provides $\tau_c \geq 0.5$ milliseconds and $T_s \geq -4^\circ$C, so a fair comparison between both cooling techniques may not be possible, as it would imply artificially increasing τ_c and T_s for CSC, or decreasing those values for SCC.

Using the SCS-SLP approach, it is expected that patients with fair skin types (I–IV) would benefit if CSC nozzle devices could provide and maintain η in the order of 80%, i.e., $h \geq 10{,}000$ W/m^{2}K. In recent studies [8,9], we measured an h value as high as 40,000 W/m^{2}K [9] for a spray produced by a 1.4 mm diameter nozzle. This h value corresponds to $\eta \approx 90\%$. However, this experiment consisted of a continuous spray aimed at a thin copper rod, and it may not necessarily represent a realistic estimate for short cryogen spurts. Furthermore, as the temperature profiles presented in Figure 3 suggest, there is an upper limit to the expected benefit in PWS laser therapy based solely on maximization in CSC, and for h values $\geq 30{,}000$ W/m^{2}K there is a negligible impact on the underlying skin temperature.

Alternatively, and considering the configurations and simplifications intrinsic to the numerical model developed for this study, the MCS-MLP approach provides the necessary epidermal protection for darker skin types V–VI, while achieving sufficient thermal confinement within PWS vessels. Note that this approach provides adequate treatment even for configuration 2 (50 μm thick PWS vessel, 300 μm deep), which represents a more challenging scenario because smaller PWS vessels diffuse heat more rapidly. Our computations show that this situation is overcome by slightly reducing the multiple cryogen spurts duration from 60 to 50 microseconds, which increases the laser pulse repetition rate. However, since this change also induces further heating of the epidermis, the η has to be increased to provide adequate epidermal protection. This was achieved by changing the value of h from 10,000 to 30,000 [W/m^{2}K], which is clearly approaching an ideal η. Therefore, it is fair to say that even though MCS-MLP may represent a significant improvement to the current SCS-SLP approach, it may still be inadequate to photocoagulate small PWS vessels, particularly shallow ones.

For all our computations we modified the values for h and T_c after the last cryogen spurt to represent a more realistic scenario in which condensed and frozen water melt steadily on the skin surface. However, other boundary conditions could also apply. For example, values of $h = 1{,}000$ W/m^{2}K and $T_c = -26^\circ$C could be used to simulate a thin liquid layer of boiling cryogen. Alternatively, values of $h = 10$ W/m^{2}K and $T_c = 25^\circ$C could simulate a steady air atmosphere at room temperature. Our experience indicates that the magnitude of h and T_c during and after the cryogen spurt is a function of nozzle geometry, nozzle-to-skin distance, and τ_c. Thus, the magnitudes of h and T_c used for computer simulations should be related to a specific nozzle device and CSC procedure. For example, it is not clear whether the Robin boundary condition with constant values of T_c and h is a valid approximation for nozzles that produce relatively thick cryogen layers on the skin surface. This is particularly true for $\tau_c > 100$ milliseconds and for nozzles which produce finely atomized sprays [9].

In addition to the appropriate quantification of the instantaneous boundary conditions, variations of skin thermal properties with temperature may be very important if cutaneous water freezes during CSC, which is more likely to occur during longer spurts (e.g., 300 milliseconds). This could have a significant impact on heat extraction from skin, as it involves a significant storage of latent heat [18].

Values of Ω_E and Ω_{PWS} reported in this study correspond to depths where maximum thermal damage occurred. Interestingly, it should be noted that during the MCS-MLP approach, the site of maximal temperature is not the same within the PWS, as seen in Figures 6 and 7. Depending on thickness and depth of the PWS vessels, CSC boundary condition, and the MCS-MLP parameters, it appears that the maximum temperature within the PWS vessel (and therefore maximum Ω_{PWS}) can shift from the bottom edge of the PWS vessel towards its upper edge and back to the bottom edge, as in Figure 6b, or continuously shift from the back edge to the upper, as in Figure 7b.

A current commercial laser device (Vbeam^{TM}; Candela Corporation, Wayland, MA) is capable of delivering multiple 595 nm wavelength laser pulses at a maximum of 1.5 Hz with fluences as high as 25 J/cm^2. Another commercial device (Smoothbeam^{TM}; Candela Corporation) delivers multiple cryogen spurts intermittently with multiple 1450 nm laser pulses. However, the hemoglobin and oxy-hemoglobin absorptions are very low at this wavelength and, also, the repetition rate between the multiple cryogen spurts and laser pulses (1 Hz) is not as fast as required for the MCS-MLP approach discussed herein.

According to our results, if pulse repetition rates could be increased to ~ 16–20 Hz (to permit epidermal cooling) for a device similar to the Vbeam with a 595 nm wavelength, the number of multiple pulses adjusted to ~ 10–25 (to increase energy absorption in the blood vessels), and multiple 50–60 milliseconds cryogen spurts were delivered intermittently with each laser pulse, the efficacy of PWS laser therapy would be expected to increase significantly, especially for patients with darker skin types. In any event, the application of the MCS-MLP approach and the validity of the predicted thermal damages must still be supported by experimental evidence and histological measurements of human skin, respectively. These are the objectives of ongoing work, which will be reported shortly.

CONCLUSIONS

A new definition to compute η of CSC on human skin has been proposed. With this definition, it is possible to estimate that η of current nozzle devices varies between 40 and 98%. Improvements in CSC that lead to h values beyond 30,000 W/m^{2}K will not have a significant impact on η, since the thermal resistance of human skin becomes the limiting factor for determining the rate of heat extraction.

Using heat diffusion, light distribution, and thermal damage computational models, it is shown that patients with darker skin types (e.g., V–VI) are not suitable candidates for PWS treatment using a single cryogen spurt and single 585–595 nm pulsed-dye laser exposure (SCS-SLP approach), regardless of η. However, multiple-intermittent cryogen spurts and laser pulses (MCS-MLP approach) could provide adequate epidermal protection while inducing the desired PWS vessel damage for patients with skin types V–VI. The validity of the MCS-MLP approach should be eventually confirmed through clinical trials and histological characterization.

ACKNOWLEDGMENTS

Institutional support from the Office of Naval Research, Department of Energy, National Institutes of Health, and the Beckman Laser Institute Endowment is acknowledged. Useful discussions with Dr. J.A. Viator and Dr. B. Choi are appreciated.

REFERENCES

1. Nelson JS, Milner TE, Anvari B, Tanenbaum BS, Kimel S, Svaasand LO, Jacques SL. Dynamic epidermal cooling during pulsed laser treatment of port-wine stain. Arch Dermatol 1995;131:695–700.
2. Chang CJ, Nelson JS. Cryogen spray cooling and higher fluence pulsed dye laser treatment improve port wine stain clearance while minimizing epidermal damage. Dermatol Surg 1999;25:766–771.
3. Morelli JG, Weston WL, Huff JC, Yohn JJ. Initial lesion size as a predictive factor in determining the response of port-wine stains in children treated with the pulsed dye laser. Arch Pediatr Adolesc Med 1995;149:1142–1144.
4. Van der Horst CMAM, Koster PHL, deBorgie CAJM, Bossuyt PMM, van Gemert MJC. Effect of timing of treatment of port-wine stains with the flash-lamp-pumped pulsed dye laser. N Engl J Med 1998;338:1028–1033.
5. Fitzpatrick TB. The validity and practicality of sun-reactive skin types I through VI. Arch Dermatol 1988;124:869–871.
6. Verkruysse W, Majaron B, Tanenbaum BS, Nelson JS. Optimal cryogen spray cooling parameters for pulsed laser treatment of port wine stains. Lasers Surg Med 2000;27:165–170.
7. Tunnell JW, Nelson JS, Torres JH, Anvari B. Epidermal protection with cryogen spray cooling during high fluence pulsed dye laser irradiation: An ex vivo study. Lasers Surg Med 2000;27:373–383.
8. Verkruysse W, Majaron B, Aguilar G, Svaasand LO, Nelson JS. Dynamics of cryogen deposition relative to heat extraction rate during cryogen spray cooling. Proc SPIE 2000;3907: 37–48.
9. Aguilar G, Verkruysse W, Majaron B, Svaasand LO, Lavernia EJ, Nelson JS. Measurement of heat flux and heat transfer coefficient during continuous cryogen spray cooling for laser dermatologic surgery. IEEE J Sel Top Quant 2001; 7:1013–1021.
10. Anvari B, Ver Steeg BJ, Milner TE, Tanenbaum BS, Klein TJ, Gerstner E, Kimel S, Nelson JS. Cryogen spray cooling of human skin: Effects of ambient humidity level, spraying distance, and cryogen boiling point. Proc SPIE 1997;3192: 106–110.
11. Aguilar G, Majaron B, Pope K, Svaasand LO, Lavernia EJ, Nelson JS. Influence of nozzle-to-skin distance in cryogen spray cooling for dermatologic laser surgery. Lasers Surg Med 2001;28:113–120.
12. Majaron B, Aguilar G, Basinger B, Randeberg LL, Svaasand LO, Lavernia EJ, Nelson JS. Sequential cryogen spraying for heat flux control at the skin surface. Proc SPIE 2001;4244: 74–81.
13. Torres JH, Tunnell JW, Pikkula BS, Anvari B. Cryogen spray cooling for dermatological laser therapy. Dynamics of cryogen deposition and effect of simultaneous airflow application. Lasers Surg Med 2001;28:477–486.
14. Tan OT, Hurwitz RM, Stafford TJ. Single or multiple pulses in the use of the pulsed dye laser for the treatment of port-wine stains. Lasers Med Sci 1996;11:205–210.
15. Anvari B, Tanenbaum BS, Milner TE, Tang K, Liaw LH, Kalafus K, Kimel S, Nelson JS. Spatially selective photocoagulation of biological tissues—feasibility study utilizing cryogen spray cooling. Appl Opt 1996;35:3314–3320.
16. Anvari B, Tanenbaum BS, Hoffman W, Said S, Milner TE, Liaw LH, Nelson JS. Nd:YAG laser irradiation in conjunction with cryogen spray cooling induces deep and spatially selective photocoagulation in animal models. Phys Med Biol 1997; 42:265–282.
17. Aguilar G, Majaron B, Verkruysse W, Nelson JS, Lavernia EJ. Characterization of cryogenic spray nozzles with application to skin cooling. Proc ASME 2000;FED-253:189–197.
18. Majaron B, Kimel S, Verkruysse W, Aguilar G, Pope K, Svaasand LO, Lavernia EJ, Nelson JS. Cryogen spray cooling in laser dermatology: Effects of ambient humidity and frost formation. Lasers Surg Med 2001;28:469–476.
19. Anvari B, Milner TE, Tanenbaum BS, Kimel S, Svaasand LO, Nelson JS. Selective cooling of biological tissues: Application for thermally mediated therapeutic procedures. Phys Med Biol 1995;40:241–252.
20. Torres JH, Nelson JS, Tanenbaum BS, Milner TE, Goodman DM, Anvari B. Estimation of internal skin temperature measurements in response to cryogen spray cooling: Implications for laser therapy of port wine stains. IEEE J Sel Top Quant 1999;5:1058–1066.
21. Aguilar G, Majaron B, Viator JA, Basinger B, Karapetian E, Svaasand LO, Lavernia EJ, Nelson JS. Influence of spraying distance and post-cooling on cryogen spray cooling for dermatologic laser surgery. Proc SPIE 2001;4244:82–92.
22. Incropera FP, DeWitt DP. Fundamentals of Heat and Mass Transfer. 4th Edn. New York: John Wiley & Sons; 1996. p. 238–239.
23. Duck FA. Thermal properties of tissue. In: Physical properties of tissue. London: Academic press; 1990.
24. van Gemert MJC, Welch AJ, Pickering JW, Tan OT. Laser treatment of port wine stains. In: Welch AJ, van Gemert MJC, editors. Optical-thermal response of laser irradiated tissue. New York: Plenum Press; 1995.
25. Pfefer TJ, Smithies DJ, Milner TE, van Gemert MJC, Nelson JS, Welch AJ. Bioheat transfer analysis of cryogen spray cooling during laser treatment of port wine stains. Lasers Surg Med 2000;26:145–157.
26. Jacques SL, Glickman RD, Schwartz JA. Internal absorption coefficient and threshold for pulsed laser disruption of melanosomes isolated from retinal pigment epithelium. Proc SPIE 1996;2681:468–477.
27. Verkruysse W, Pickering JW, Beek JF, Keijzer M, van Gemert MJC. Modeling the effect of wavelength on the pulsed dye laser treatment of port wine stains. Appl Opt 1993;32: 393–398.
28. Oregon Medical Laser Center (OMLC). 2001. Website, http://omlc.ogi.edu/spectra/melanin/index, visited on March 23, 2001.
29. Jacques SL. 2001. Personal communication. Beckman Laser Institute and Medical Clinic, Irvine CA, May 7, 2001.
30. Wang LH, Jacques SL, Zheng LQ. MCML—Monte Carlo modeling of light transport in multi-layered tissues. Comp Meth Prog Bio 1995;47:131–146.
31. Wang LH, Jacques SL, Zheng LQ. CONV—Convolution for responses to a finite diameter photon beam incident on multi-layered tissues. Comp Meth Prog Biol 1997;54:141–150.
32. Smithies DJ, van Gemert MJC, Hansen MK, Milner TE, Nelson JS. Three-dimensional reconstruction of port wine stain vascular anatomy from serial histological sections. Phys Med Biol 1997;42:1843–1847.